Characterization of the Tryptophan Binding Site of *Escherichia coli* Tryptophan Holorepressor by Phosphorescence and Optical Detection of Magnetic Resonance of a Tryptophan-Free Mutant†

Zhi Li,‡ August H. Maki,*,‡ Maurice R. Eftink,§ Craig J. Mann,|| and C. R. Matthews||

Department of Chemistry, University of California, Davis, California 95616, Department of Chemistry, University of Mississippi, University, Mississippi 38677, and Department of Chemistry, Pennsylvania State University, University Park, Pennsylvania 16802

Received February 24, 1995; Revised Manuscript Received June 27, 1995⊗

ABSTRACT: The L-tryptophan binding site of the *Escherichia coli* tryptophan holorepressor (trpR) is characterized by low-temperature phosphorescence and optical detection of magnetic resonance (ODMR) spectroscopy. Measurements are made on a tryptophan-free mutant of trpR, W19/99F, in which both intrinsic tryptophan residues of apo-trpR have been replaced with phenylalanine. Thus, essentially all of the phosphorescence that is observed from trpR originates from the bound L-tryptophan corepressor. The phosphorescence and ODMR results for the bound corepressor agree quite well with those obtained previously for the corepressor site in both single tryptophan-containing mutants, W19F and W99F [Burns, L. E., & Maki, A. H. (1994) *J. Fluorescence 4*, 217−226]. A red shift of the L-tryptophan phosphorescence origin as well as a decrease in the D-E ODMR frequency result from an increase in the local polarizability upon binding at the corepressor binding site. A large decrease in the ODMR line widths signals a reduction of local heterogeneity upon binding. Subsequent binding of trpR to a self-complementary DNA sequence that mimics the *trp* operator, 5′-CGTACTAGTTAACTAGTACG-3′, produces a further decrease in line widths and additional changes in the ODMR frequencies, attributable to an increase in both the D and E parameters. This result demonstrates that binding of holo-trpR to the operator affects the local environment of the bound corepressor.

Tryptophan aporepressor (apo-trpR)[1] from *Escherichia coli* is a symmetrical dimeric protein that contains two tryptophan residues per 107 amino acid subunit at positions 19 and 99 (Zhang et al., 1987). The active holoprotein, trpR, is formed upon noncooperative binding of two molecules of the corepressor, L-tryptophan, to apo-trpR, whereupon it binds selectively to at least four sites on the *E. coli* genome, the *trp*, *aroH*, *mtr*, and *trpR* operons, to regulate the expression of genes involved in tryptophan synthesis and transport (Bennett & Yanofsky, 1978; Gunsalus & Yanofsky, 1980; Zurawski et al., 1981; Joachimiak et al., 1983; Arvidson et al., 1986; Marmorstein et al., 1987). TrpR has been investigated extensively as a model for the general behavior of regulatory proteins (Platt, 1980; Sommerville, 1983). The apo-trpR subunit contains six α-helixes, four of which fold into a hydrophobic core, while the remaining two helixes form helix−turn−helix DNA-binding domains (Zhang et al., 1987). L-trp binds independently to each subunit in a hydrophobic pocket located between the core and the DNA-binding domain (Shevitz et al., 1985). The presumed role of the bound corepressor is to induce a conformational change in apo-trpR such that the reading heads of the dimer can penetrate two successive grooves of the operator (Arnott & Hukins, 1972). Bound L-trp apparently does not lock trpR into a single conformation corresponding to the *trp* operator but probably leaves it sufficiently flexible to regulate the remaining operons as well (Lawson et al., 1988).

Previous fluorescence measurements of the binding of L-trp to wild-type apo-trpR (Lane, 1985) revealed a large blue shift, confirming the hydrophobic and nonpolar nature of the corepressor binding site as deduced from the X-ray crystallographic results (Shevitz et al., 1985). The fluorescence emission of Trp is too broad and unstructured to effectively separate that of the corepressor and intrinsic residues. More recently, Millar et al. (1992) have isolated the corepressor fluorescence of trpR by utilizing a tryptophan-free mutant of apo-trpR, W19L/W99M, in which Trp19 and Trp99 are replaced with leucine and methionine, respectively. These studies confirm the blue shift induced in the corepressor fluorescence (and in that of several pseudo-corepressors), but decay kinetics suggest that the binding is heterogeneous, with at least three binding modes coexisting.

In the work presented here, we have used a different tryptophan-free mutant of apo-trpR, W19/99F, to characterize the corepressor binding site using phosphorescence and optical detection of magnetic resonance (ODMR) spectroscopy. In this mutant repressor, all of the intrinsic Trp residues of apo-trpR have been substituted with phenylalanine, whose phosphorescence emission is not induced under the conditions of our measurements. In previous work

† This research was partially supported by NIH Grant ES-02622 to A.H.M. and NSF Grant MCB9407167 to M.R.E.

* Author to whom correspondence should be addressed.
‡ University of California, Davis.
§ University of Mississippi.
|| Pennsylvania State University.

⊗ Abstract published in *Advance ACS Abstracts,* August 15, 1995.

[1] Abbreviations: EDTA, ethylenediaminetetraacetic acid; MIDP, microwave-induced delayed phosphorescence; ODMR, optically detected (triplet state) magnetic resonance; SLR, spin−lattice relaxation; trpR, tryptophan repressor protein from *E. coli*; W19/99F, tryptophan-free mutant of trpR employed in these measurements; zfs, zero-field splittings.

0006-2960/95/0434-12866$09.00/0 © 1995 American Chemical Society

(Eftink et al., 1993) we have studied the luminescence and ODMR properties of two single-tryptophan mutants of apo-trpR, W19F and W99F, in order to characterize the intrinsic Trp residues. These mutated proteins were employed subsequently (Burns & Maki, 1994) in phosphorescence and ODMR measurements of holo-trpR. Because of the highly resolved character of Trp phosphorescence, we were able to discriminate between the bound corepressor and intrinsic Trp ODMR and phosphorescence spectra in these single-tryptophan proteins by using wavelength selection methods. In this work, we found a red shift in the phosphorescence emission of L-trp upon binding at the corepressor site, a large decrease in its D-E ODMR frequency, and a substantial reduction in ODMR line widths, all characteristic of binding at a more polarizable and homogeneous site. The present work was undertaken to verify and to improve on these previous results by using a mutated apo-trpR in which interference from intrinsic Trp emission would be effectively eliminated, and to extend these measurements to a complex of trpR with a DNA operator sequence.

MATERIALS AND METHODS

A tryptophan-free mutant of apo-trpR, W19/99F, in which the two intrinsic Trp residues are replaced with phenylalanine was used in our measurements. The preparation of this mutant by site-directed mutagenesis is described elsewhere (Mann et al., 1993). A self-complementary mimic of the *trp* operator, 5′-dCGTACTAGTTAACTAGTACG-3′, was synthesized and purified by Midland Certified Reagent Co. (Midland, TX). The apo-trpR sample was stored as a suspension in 70% ammonium sulfate and was dialyzed into 0.1 M potassium phosphate buffer, pH 7.0, containing 5 mM EDTA. L-Tryptophan was obtained from Fluka and was used without further purification. Spectrophotometric-grade glycerol was purchased from Aldrich. The solvent used in the low-temperature spectroscopic measurements was prepared by mixing glycerol with buffer in a ratio of 30:70 (v/v). The final protein concentration was determined from the optical density measured at 280 nm based on $\epsilon_{280} = 4800\ M^{-1}\ cm^{-1}$. DNA concentrations were calculated using an average ϵ_{260} of $1 \times 10^4\ M^{-1}\ cm^{-1}$ per nucleotide for single-stranded DNA (Cantor & Schimmel, 1980) and reducing it by the factor 0.73 to account for hypochromicity in forming a duplex.

The optical excitation source for phosphorescence and ODMR measurements was a 100-W Hg high-pressure short-arc lamp. The excitation wavelength was selected by a 0.1-m grating monochromator (Instruments SA, Inc.) using a 16-nm band pass. The sample, contained in a 1-mm i.d. Suprasil quartz tube, was placed within a copper helix that terminated a section of 50-Ω coaxial transmission line. The latter was immersed in a cryostat (Janis, Inc., Model 8DT) fitted with an optical tail in which the sample could be maintained either at ca. 77 K for phosphorescence measurements or at the temperature of pumped liquid He, ca. 1.2 K, for slow-passage ODMR and MIDP measurements. Emission from the sample was monitored at a 90° angle with respect to excitation and was focused on the entrace slit of a 1-m grating monochromator (McPherson, Inc., Model 2051) with a dispersion of 3.2 nm/mm. For phosphorescence spectra and slow-passage ODMR measurements, fluorescence and scattered light were suppressed by a rotating sector. A 345-nm cutoff filter was always present in the emission path. The optical signals were detected by an EMI, Inc., Model 6256, blue-sensitive photomultiplier tube maintained at −5 °C and placed at the monochromator exit slit. The photomultiplier output was amplified using a Keithley, Inc., Model 427 current amplifier. The signals were averaged and stored in a signal-averaging computer (Tracor-Northern, Model TN1550) that was interfaced with an IBM-compatible personal computer.

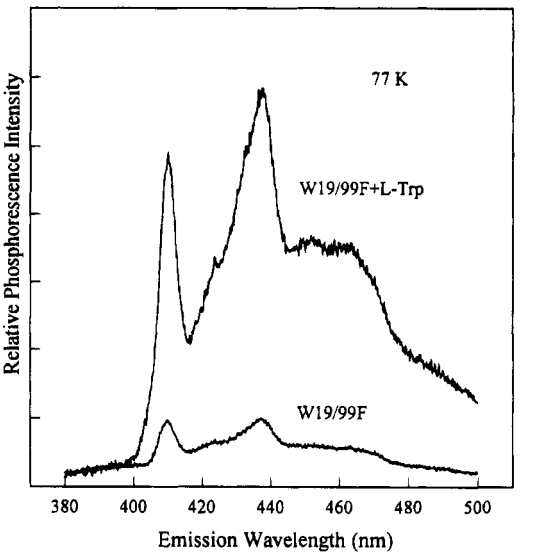

FIGURE 1: Phosphorescence spectra of the tryptophan-free mutant, W19/99F, and of its complex with L-trp. Samples are excited at 296 nm. The protein concentration in each sample is 8×10^{-5} M expressed as monomer, and the concentration of L-trp is 5×10^{-5} M.

Experimental details of slow-passage ODMR and MIDP measurements have been discussed in recent reviews (Hoff, 1994; Maki, 1995). The instrumentation used in our measurements has been described in previous papers (Tsao et al., 1989; Burns et al., 1993; Burns & Maki, 1994). ODMR resonance frequencies and line widths were corrected for passage effects by extrapolation to zero sweep rate. Phosphorescence decays were analyzed using a Marquardt algorithm designed to minimize χ^2.

RESULTS

Phosphorescence Spectra and Triplet State Lifetimes at 77 K. The phosphorescence spectra of W19/99F and the complex of L-trp and W19/99F (holo-trpR) are compared in Figure 1. The optimum protein to L-trp ratio was obtained by monitoring the 0,0-band region, maximizing the contribution of the bound corepressor to the phosphorescence without the appearance of a significant unbound L-trp contribution. The phosphorescence spectrum of unbound L-trp (not shown) exhibits a 0,0-band peak at 406.6 nm with excitation centered at 296 nm (condition used to obtain the spectra shown in Figure 1). It is found more than 2 nm to the blue of the prominent 0,0-band exhibited by the holo-trpR in Figure 1 (408.9 nm). The holo-trpR spectrum was obtained with L-trp and W19/99F concentrations of 5×10^{-5} and 8×10^{-5} M, respectively. Increasing the concentration of L-trp beyond 5×10^{-5} M resulted initially in an obvious broadening on the blue edge of the 0,0-band and an eventual shifting of the 0,0-band maximum to the blue. This is attributed to the accumulation of free L-trp in the sample. Under the conditions of Figure 1, there is insignificant contribution of free L-trp to the emission when monitored at the 0,0-band peak of 408.9 nm.

Table 1: Tryptophan Phosphorescence 0,0-Band Peak Wavelength and Decay Analysis[a]

sample	$\lambda_{0,0}$ (nm)	lifetimes[b] (s)	
L-trp	406.6	6.9 (100)	
W19/99F + L-trp	408.9	6.5 (88)	0.5 (12)
W19/99F + L-trp + DNA	410.0	6.4 (71)	0.4 (28)

[a] $T = 77$ K. Samples are dissolved in 0.1 M phosphate buffer, pH 7.0, containing 30% (v/v) glycerol. Uncertainties in λ and lifetimes are ±0.3 nm and ±0.1 s, respectively. [b] Initial amplitudes, in percent, are in parentheses.

It is clear that there is a contribution of Trp to the phosphorescence of W19/99F (Figure 1). This emission could have a number of origins. It could originate from a tryptophan-containing protein contaminant of W19/99F. Also, it is possible that the mutated apo-trpR could contain a small amount of holo-trpR. The latter explanation is suggested by the fact that the peak 0,0-band wavelength of the "impurity" phosphorescence is the same as that attributed to the bound corepressor within measurement error (see Figure 1). Then again, it differs significantly from the 0,0-band peak wavelengths found for Trp 19 and Trp 99 of apo-trpR in the single tryptophan-containing mutants, 407.5 and 414.5 nm, respectively (Burns & Maki, 1994). Whatever its origin, we find that its emission is weak when compared with that of the bound corepressor, and we estimate that its contribution to the emission intensity of the holo-trpR sample at 408.9 nm does not exceed 10%.

Addition of the oligonucleotide operator mimic produced a small but significant red shift of the 0,0-band of trpR (spectrum not shown), confirming that the holorepressor binds to the operator analog. The 0,0-band wavelengths of L-trp, holo-trpR, and the holo-trpR complex with the operator mimic are presented in Table 1. In all of our measurements, the concentrations of L-trp, W19/99F, and DNA operator mimic were 5×10^{-5}, 8×10^{-5}, and 4×10^{-4} M, respectively, each expressed as monomer. The phosphorescence decay of L-trp when monitored at its 0,0-band peak was found to be a single exponential, while that of holo-trpR and its complex with the operator analog could be fit well to two exponential components. The phosphorescence decays of holo-trpR and its complex with the operator analog are compared in Figure 2. The decay lifetimes obtained from the analyses are given in Table 1. The short component observed in the decay of trpR probably originates largely from tyrosine, while that of the trpR complex with the *trp* operator mimic may contain a component of DNA phosphorescence, as well.

ODMR Results and Individual Triplet Sublevel Kinetics. Slow-passage ODMR spectra were obtained using phosphorescence detection at 1.2 K with the emission monitored at the 0,0-band wavelengths given in Table 1. The spectra of L-trp, trpR, and the trpR complex with the operator mimic are shown in Figure 3. The two signals observed are the D-E and 2E zfs transitions; they are found at frequencies that are typical for the triplet state of Trp. The binding of L-trp to the corepressor binding site leads to an increase in the 2E frequency and a decrease in the D-E frequency (Figure 3). In addition, the ODMR line widths are significantly reduced when L-trp binds to the corepressor binding site. When holo-trpR binds to the *trp* operator mimic, there is a further increase in the 2E frequency of the bound corepressor (Figure 3). The ODMR frequencies, line widths, and the zfs D and E parameters for the three samples investigated are presented in Table 2.

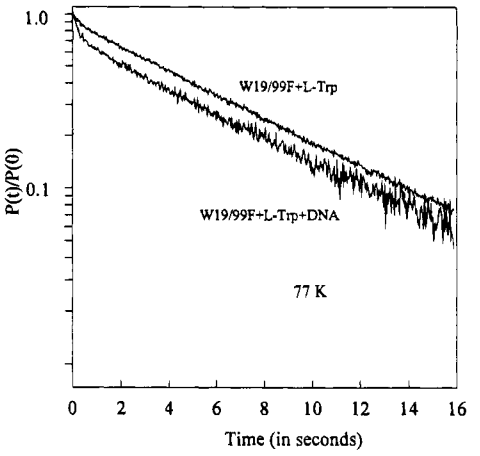

FIGURE 2: Semilogarithmic plots of the phosphorescence decays of the holorepressor formed from W19/99F and L-trp and its complex with the *trp* operator mimic. The concentrations of W19/99F and L-trp are as given in the caption of Figure 1. The oligonucleotide concentration is ca. 5.5×10^{-4} M. The decay was monitored at the respective 0,0-band peak wavelengths given in Table 1 using 3-nm band pass.

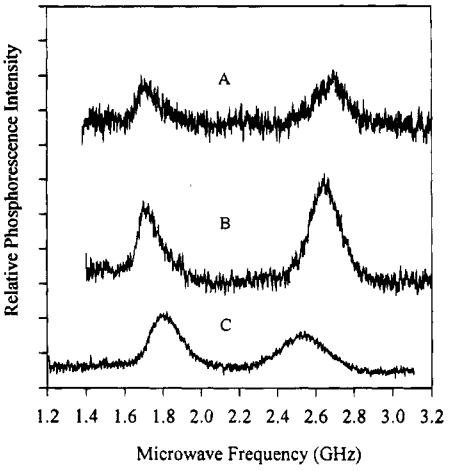

FIGURE 3: Phosphorescence-detected slow-passage ODMR signals of tryptophan in the various samples: (A) W19/99F + L-trp + *trp* operator mimic, (B) W19/99F + L-trp, and (C) free L-trp. The temperature is 1.2 K, and the phosphorescence is monitored at the respective 0,0-band peaks given in Table 1 using 3-nm band pass. Concentrations are given in the captions of Figures 1 and 2. The microwave frequency was swept at 36 MHz/s and signal averaging was carried out to improve the signal/noise.

Table 2: Tryptophan ODMR Frequencies and zfs Parameters[a]

sample	$\nu_{D\text{-}E}$[b] (GHz)	ν_{2E}[b] (GHz)	D (GHz)	E (GHz)
L-trp	1.77 (128)	2.49 (217)	3.02	1.25
W19/99F + L-trp	1.68 (89)	2.60 (163)	2.98	1.30
W19/99F + L-trp + DNA	1.68 (48)	2.66 (107)	3.01	1.33

[a] $T = 1.2$ K. Samples are monitored at the 0,0-band peak (Table 1) with 3-nm band pass. Uncertainty in ODMR frequencies and zfs parameters is ±0.01 GHz. [b] Line widths, full width at half-maximum intensity, in megahertz, are in parentheses.

Triplet sublevel kinetics were obtained from MIDP measurements; a typical example is shown in Figure 4 in which 2E transition-induced phosphorescence transients of holo-trpR and its complex with the operator analog are shown. The insert shows semilog plots of the intensity of

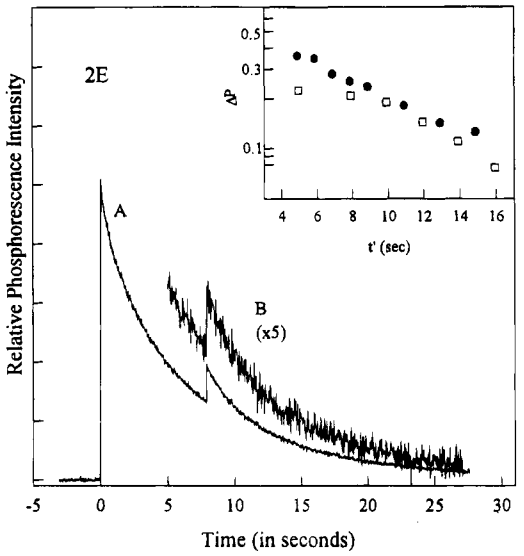

FIGURE 4: MIDP responses induced by the tryptophan 2E transition in (A) the active trpR formed from W19/99F and L-trp and (B) its complex with the *trp* operator mimic. Concentrations are as given in the captions of Figures 1 and 2; the emission is monitored as described in the Figure 3 caption. The inset gives a semilogarithmic plot of the intensity of the microwave-induced response, ΔP, vs t', the time delay between shuttering the optical excitation and the microwave sweep. The open squares and solid circles denote the binary and ternary complexes, respectively.

Table 3: Apparent Triplet Sublevel Decay Constants of Tryptophan Obtained from MIDP Measurements[a]

sample	k_x[b] (s^{-1})	k_y (s^{-1})	k_z (s^{-1})	k_{av}[c] (s^{-1})
L-trp	0.30	0.082 ± 0.003	0.037 ± 0.002	0.14
W19/99F + L-trp	0.28	0.10 ± 0.01	0.070 ± 0.004	0.15
W19/99F + L-trp + DNA	0.33	0.14 ± 0.01	0.087 ± 0.007	0.19

[a] $T = 1.2$ K. Samples are monitored at the 0,0-band peak using 3-nm band pass. [b] Uncertainty is ± 0.01 s^{-1}. [c] Average decay constant $k_{av} = (k_x + k_y + k_z)/3$.

the induced transient from which the apparent decay constant[2] of the T_y sublevel is obtained. (The 2E transition connects the radiative T_x sublevel and the nonradiative T_y sublevel.) The decay constant of the radiative T_x sublevel is obtained by deconvolution of the transient itself. The apparent decay constant of the T_z sublevel is obtained by a similar analysis of the MIDP given by the D-E transition that connects T_x and T_z [see, for instance, Tsao et al. (1989)]. The apparent sublevel decay constants of the three samples investigated are presented in Table 3. The changes observed in the triplet-state sublevel kinetics of Trp in its various environments are relatively small and seem to manifest themselves mostly in the smaller apparent decay constants, k_y and k_z, which increase when L-trp is first bound to the corepressor binding site, and increase again as trpR is bound to the *trp* operator mimic. DNA binding of trpR also appears to lead to an increase in k_x.

[2] We refer to the decay constants as measured in the MIDP experiments as "apparent decay constants" since they may not be the simple result of decay of the sublevel population to the ground singlet state but may be influenced by residual spin−lattice relaxation (SLR) processes that are not totally quenched even at 1.2 K. If SLR is effectively quenched, these rate constants represent simple decay to S_0.

DISCUSSION

We have used the tryptophan-free mutated apo-trpR, W19/99F, to provide spectroscopic data relating to L-trp bound at the corepressor binding site. In addition, we have investigated the effects of binding a DNA oligomer mimic of the *trp* operator on the bound corepressor. Our measurements have focused on the properties of the triplet state of the bound L-trp, which we have studied using phosphorescence and ODMR spectroscopy. The W19/99F mutant allowed us to effectively eliminate interfering emission from the intrinsic Trp residues of the wild-type protein. This work is a continuation of earlier phosphorescence and ODMR measurements on two single-tryptophan-containing mutants of apo-trpR that allowed us to partially characterize L-trp bound to the corepressor binding site (Burns & Maki, 1994). The present results agree well with those obtained in the earlier work and enable the unambiguous characterization of the triplet-state properties of bound L-trp. A tryptophan-free mutant of apo-trpR also has been employed previously by Millar et al. (1992) in order to isolate the fluorescence of bound L-trp and that of several indole-containing corepressor analogs.

The principal effects of binding L-trp in the corepressor binding site on the triplet-state properties are a red shift of the phosphorescence origin of ca. 2.3 nm, an increase in the zfs E parameter, a decrease in D, and a significant reduction in the ODMR line widths. The effects of binding on the zfs parameters and ODMR line widths, as well as the phosphorescence red shift, characterize the binding site as one of reduced heterogeneity and increased polarizability relative to the bulk solvent (Purkey & Galley, 1970; Hershberger et al., 1980). In a rigid medium, polar solvent molecules remain oriented in positions that stabilize the ground-state electronic distribution when the excited state, with a differing distribution, is formed. Thus, polar solvent environments lead to a blue shift of the phosphorescence spectrum. Polarizable, nonpolar environments, on the other hand, stabilize the excited triplet state (which in indole has the larger dipole moment) more than the ground state, leading to a red shift of the phosphorescence. The spectroscopic properties that we observe are in accord with the X-ray crystal structure data on trpR (Shevitz et al., 1985). The indole ring of L-trp is sandwiched between the aliphatic side chains of two arginine residues of one subunit while the carboxylate and ammonium groups of the alanyl side chain form hydrogen bonds with amino acid residues in the other subunit of the trpR dimer. The hydrocarbon environment of the indole chromophore of the corepressor within trpR is more polarizable than the aqueous solvent environment of L-trp. The protein structure also provides a more homogeneous environment than is provided by the polar solvent.

When trpR is bound to the *trp* operator mimic, both D and E of the bound L-trp increase and the ODMR line widths are reduced even further. There is also a small (ca. 1.1 nm) additional red shift of the phosphorescence origin. These spectroscopic changes confirm that the bound corepressor is involved in the interaction of trpR with the DNA operator mimic. The crystal structure of trpR complexed with a *trp* operator mimic has been determined at atomic resolution (Otwinowski et al., 1988). There are no direct hydrogen bonds or nonpolar contacts between the DNA bases and the trpR. Binding occurs through 24 direct and 6 solvent-

mediated hydrogen bonds between trpR and the DNA backbone, suggesting that sequence specificity arises from the indirect influence of base sequence on the external sugar−phosphate structure. The indole N−H of the corepressor is hydrogen-bonded to a specific phosphate of the *trp* operator mimic. It is probably this interaction that is largely responsible for the spectroscopic changes described above. The approach of the negatively charged phosphate induces changes in the internal charge distribution of the chromophore that results in the red shift and changes in the zfs parameters. It is interesting that the bound L-trp corepressor has the smallest thermal parameters of any residue in the structure (Otwinowski et al., 1988) as a result of strong contacts with the protein and DNA. This suggests that it resides in a very homogeneous environment in the trpR−operator complex resulting in the observed ODMR line narrowing.

REFERENCES

Arnott, S., & Hukins, D. W. L. (1972) *Biochem. Biophys. Res. Commun. 47*, 1504−1509.

Arvidson, D. N., Bruce, C., & Gunsalus, R. P. (1986) *J. Biol. Chem. 261*, 238−243.

Bennett, G. N., & Yanofsky, C. (1978) *J. Mol. Biol. 121*, 179−192.

Burns, L. E., & Maki, A. H. (1994) *J. Fluorescence 4*, 217−226.

Burns, L. E., Maki, A. H., Spotts, R., & Matthews, K. S. (1993) *Biochemistry 32*, 12821−12829.

Cantor, C. R., & Schimmel, P. R. (1980) *Biophysical Chemistry. Part II: Techniques for the Study of Biological Structure and Function*, p 384, W. H. Freeman, San Francisco, CA.

Eftink, M. R., Ramsay, G. D., Burns, L. E., Maki, A. H., Mann, C. J., Matthews, C. R., & Ghiron, C. (1993) *Biochemistry 32*, 9189−9198.

Gunsalus, R. P., & Yanofsky, C. (1980) *Proc. Natl. Acad. Sci. U.S.A. 77*, 7117−7121.

Hershberger, M. V., Maki, A. H., & Galley, W. C. (1980) *Biochemistry 19*, 2204−2209.

Hoff, A. J. (1994) *Methods Enzymol. 227*, 290.

Joachimiak, A., Kelly, R. L., Gunsalus, R. P., Yanofsky, C., & Sigler, P. B. (1983) *Proc. Natl. Acad. Sci. U.S.A. 80*, 668−672.

Lane, A. N. (1985) *Eur. J. Biochem. 157*, 405−413.

Lawson, C. L., Zhang, R.-G., Shevitz, R. W., Otwinowski, Z., Joachimiak, A., & Sigler, P. B. (1988) *Proteins: Struct., Funct., Genet. 3*, 18−21.

Maki, A. H. (1995) *Methods Enzymol. 246*, 610−638.

Mann, C. J., Royer, C. A., & Matthews, C. R. (1993) *Protein Sci. 2*, 1853−1861.

Marmorstein, R. Q., Joachimiak, A., Sprinzl, M., & Sigler, P. B. (1987) *J. Biol. Chem. 262*, 4922−4927.

Millar, D., Hochstrasser, R., Chapman, D., & Youderian, P. (1992) *Proc. SPIE, Intl. Soc. Opt. Eng. 1640*, 118−125.

Otwinowski, Z., Shevitz, R. W., Zhang, R.-G., Lawson, C. L., Joachimiak, A., Marmorstein, R. Q., Luisi, B. F., & Sigler, P. B. (1988) *Nature 335*, 321−329.

Platt, T. (1980) in *The Operon* (Miller, J. H., & Reznikoff, W. S., Eds.) 2nd ed., pp 263−302, Cold Spring Harbor Laboratory, Cold Spring Harbor, NY.

Purkey, R. M., & Galley, W. C. (1970) *Biochemistry 9*, 3569−3575.

Shevitz, R. W., Otwinowski, Z., Joachimiak, A., Lawson, C. L., & Sigler, P. B. (1985) *Nature 317*, 782−786.

Sommerville, R. L. (1983) in *Amino Acid Biosynthesis and Regulation* (Hermann, K. M., & Sommerville, R. L., Eds.) pp 351−378, Addison-Wesley, Reading, MA.

Tsao, D. H. H., Casas-Finet, J. R., Maki, A. H., & Chase, J. W. (1989) *Biophys. J. 55*, 927−936.

Zhang, R.-G., Joachimiak, A., Lawson, C. L., Shevitz, R. V., Otwinowski, Z., & Sigler, P. B. (1987) *Nature 327*, 591−597.

BI950422Z